JOURNAL OF MATERIALS SCIENCE 30 (1995) 2507–2516

A study of the effects of process variables on the properties of PZT films produced by a single-layer sol–gel technique

Y. L. TU, S. J. MILNE
School of Materials, University of Leeds, Leeds LS2 9JT, UK

Thin films of $PbZr_{0.53}Ti_{0.47}O_3$ have been prepared from diol-based sols. Films up to 1 μm thick could be produced by applying a single coating on to platinized silicon substrates. A number of processing variables ranging from sol composition through to firing conditions have been examined, and their effects on film microstructure and electrical properties evaluated. Control of the lead stoichiometry was found to be of critical importance in determining dielectric and ferroelectric parameters. Values of remanent polarization and coercive field of 22–27 $\mu C\,cm^{-2}$ and 40–45 $kV\,cm^{-1}$, respectively, could be obtained by compensating for PbO lost by volatilization during firing; corresponding relative permittivity values were 800–1000.

1. Introduction

Thin films of solid-solution compositions in the $PbTiO_3$–$PbZrO_3$ system are promising candidate materials for a range of microelectronic device applications. Much of the current research activity in the subject area is devoted to developing PZT films for non-volatile memory applications. Because of the low switching voltages required for these devices, e.g. 3–4 V, films of 0.1–0.2 μm thickness are preferred. However, some other potential applications, e.g. bulk acoustic wave devices and pyroelectric detectors, require films a micrometre or more in thickness.

For multicomponent systems such as PZT, sol–gel film deposition methods have become very popular. Films are usually formed by spin-coating a substrate with an organic solution of the components and the coating is converted into a polymeric gel layer by further chemical reaction and/or solvent evaporation. The film is eventually converted to a crystalline oxide layer by firing at temperatures of 500–700 °C.

In addition to low capital costs, sol–gel routes offer the possibility of retaining the purity and chemical homogeneity of the starting sol through to the final film.

The first reports of solution methods for PT and PZT film synthesis appeared in 1984 using butanol as a solvent for lead 2 ethylhexanate, titanium tetrabutoxide and zirconium acetylacetonate [1]. Around the same time, other workers developed a route based on a sol–gel system first developed for PZT bulk gel synthesis [2]. This thin-film route used methoxyethanol as solvent for lead acetate, titanium tetrapropoxide and zirconium tetrapropoxide [3].

Most of the subsequent scientific literature on sol–gel derived PZT films relates to the methoxyethanol or MEO route, and variants thereof. The standard MEO route usually yields single-layer PT and PZT films that are up to 0.1 μm thick. Attempts to increase layer thickness beyond this value by using more concentrated and viscous solutions invariably lead to cracking. This is mainly a result of the large volume shrinkage accompanying the gel to ceramic conversion; other factors such as thermal expansion mismatches between film and substrate contribute to stresses and cracks in the coatings.

Thicker layers can be built up by repeated coating steps in which each deposited MEO gel layer is pre-fired at ~ 300 °C on a hot-plate; however, the maximum attainable multilayer thickness for crack-free films is ~ 1 μm [4].

A route based on acetic acid in place of methoxyethanol is reported to lead to single-layer PZT layers deposited on glass substrates that are up to 2.5 μm thick [5], but they were rather porous. Other workers seeking improvements to the acetic acid route imply that the thickness limit for high-quality films is around one-tenth of this value [6].

We have investigated the possibility of using various idols to produce PT and PZT precursor sols. The sols can lead to high-quality single-layer films, up to 1 μm thick [7–9]. The surface and transverse film microstructures are of a similar appearance to those produced from methoxyethanol routes [10]. As with all sol–gel routes, there are many process variables to be considered and optimized in order to develop the new diol route to its full potential.

In the present paper, we illustrate the effects of a number of important process parameters and how these can be controlled in such a way as to improve the dielectric and ferroelectric properties of $PbZr_{0.53}Ti_{0.47}O_3$ (53/47) films.

2. Experimental procedure

Gel-precursor solutions (sols) for PZT (53/47) were prepared from lead acetate trihydrate [$Pb(CH_3COO)_2 \cdot 3H_2O$], titanium diisopropoxide bisacetylacetonate

0022–2461

$[Ti(OC_3H_7)_2(CH_3COCHCOCH_3)_2]$ (TIAA), and zirconium *n*-propoxide ($Zr(O\text{-}nPr)_4$]. The solution preparation procedure is schematically shown in Fig. 1. Zirconium *n*-propoxide was first stabilized by refluxing together acetylacetone $[CH_3COCH_2COCH_3]$ (HAA) and zirconium *n*-propoxide in a 2:1 molar ratio to facilitate the exchange of *n*-propoxy for acetylacetonate groups. This zirconium complex was then mixed with TIAA and 1,3 propanediol. The mixture was heated under reflux conditions for 2 h. Lead acetate was mixed with 1,3 propanediol and then heated under refluxing conditions for 2 h to form the lead-diol precursor. These two solutions were then combined. Further reflux for 5 h with one distillation after 1 h and a second distillation after 4 h (both at 80–90 °C) yielded the gel-precursorstock solution with a concentration in excess of 1.1 M. Solutions with 10 and 20 mol % excess of $Pb(CH_3COO)_23H_2O$ were also prepared. The total ratio of diol used was 5 or 3 mol diol per mol lead. *n*-Propanol was used as the solvent to dilute the stock solution to 1 M, or 0.5 M for film deposition. Further concentration of the stock solution to 1.6 M was carried out for the deposition of a thicker single-layer film.

Lead precursor sols were prepared by heating lead acetate trihydrate and methoxyethanol under reflux for 2 h; these sols were used for the deposition of a lead oxide surface coating on selected samples. Sols of three different concentrations 1.6 M, 0.8 M and 0.4 M were prepared.

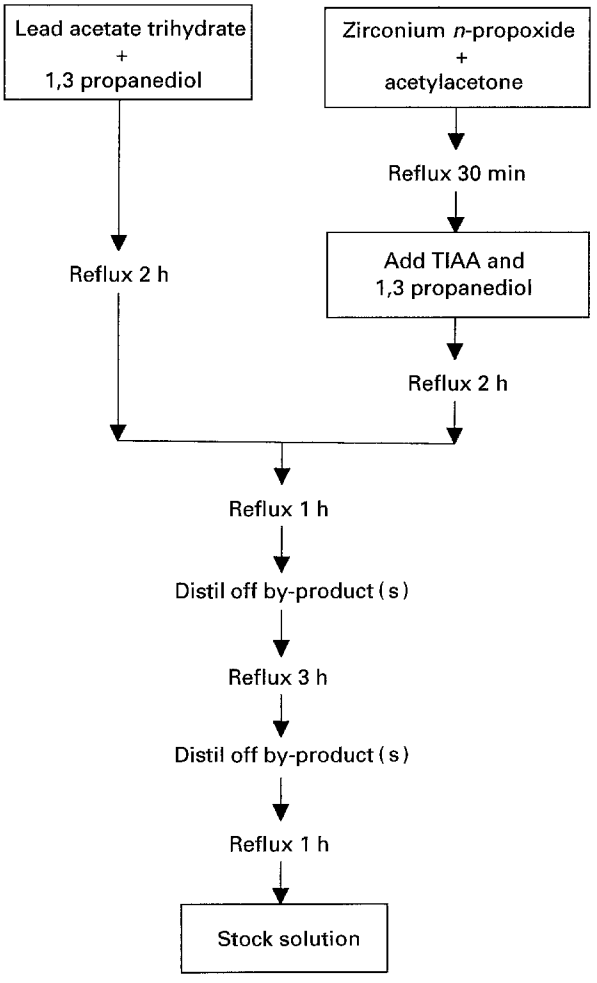

Figure 1 Flow diagram of the PZT sol synthesis process.

The kinematic viscosities of sols were measured using a Fitzsimons suspended level viscometer. Thermogravimetric analysis (TGA) was employed to monitor the decomposition of bulk gels in which volatile organic by-products had been expelled at 130 °C prior to analysis; a TGA heating rate of 5 °C min^{-1} was used.

Sols were deposited on to platinized silicon substrates having a $Pt/Ti/SiO_2/Si$ configuration. The platinum layer served as bottom electrode and was 100 nm thick, a 5 nm titanium layer acted as an adhesion layer between the platinum and the underlying silica layer. The substrates were ultrasonically cleaned in trichloroethylene followed by ultrasonic cleaning in acetone and propanol. Surplus propanol was spun off the substrates immediately prior to the deposition step. Thin films were fabricated by coating the stationery substrate with droplets of sol and spinning off the excess sol at 1500–4000 r.p.m for 1 min. The solutions were filtered through a 0.2 μm membrane filter before deposition.

The coated substrates were prefired on a hot plate at 300–450 °C for times ranging from 1–60 min. For the fabrication of films coated with a lead oxide surface layer, lead precursor solutions were spin coated on prefired coatings at 1500 r.p.m. for 1 min and then treated again at 350 °C for 1 min. Films were then fired at 700 °C in air. A direct insertion method, in which the prefired layers were inserted directly into a furnace set at the required temperature, was employed as the standard firing schedule. A thermocouple was placed beside the sample in order to monitor the heating rate and local firing temperature of this direct insertion process; the heating rate was found to be $\sim 150\,°C\,min^{-1}$.

Phase analysis of the thin films was performed at room temperature using an X-ray diffractometer (Philips APD 1700). The calculation of intensity ratios was based on peak height (c.p.s) readings. The microstructures and thickness of the PZT films were examined using scanning electron microscopy (Hitachi S700). Substrates were fractured carefully to provide a "clean" cross-section to investigate film thickness.

Thin-layer capacitors were formed by sputtering gold electrodes, using a shadow masking method, on to the top surface of the films. The gold electrodes were $\sim$ 600 μm diameter, but the exact diameter was determined using an optical microscope fitted with a calibrated graticule eyepiece. Polarization–electric field (*P–E*) characteristics were evaluated by means of a Sawyer–Tower circuit in conjunction with a Tektronics 2230 oscilloscope. A sinusoidal voltage waveform of 300 kV cm^{-1} was applied at a frequency of 60 Hz. The relative permittivity, ε_r, and dissipation factor, *D*, of the films were measured using a Hewlett Packard 4192A impedance analyser at 2 kV cm^{-1} (r.m.s) and 1 kHz. At least three measurements from different surface electrodes were taken for each sample in order to ensure that the values recorded were representative of the film as a whole. All the electrical properties were measured 10 days after firing to avoid any ageing effects.

3. Results

3.1. Film formation

The stock solutions were stable against precipitation for at least 3 months when stored in air. This high stability can be attributed to the presence of diol and acetylacetone chelating agents [11, 12] which prevent the hydrolysis and condensation of titanium and zirconium species. The viscosities of 1 M solutions prepared using diol ratios of 3 and 5 were 9×10^{-3} and 14.4×10^{-3} Pa.s, respectively.

TGA data for PZT precursor gels prepared using different diol ratios are shown in Fig. 2. As expected, total weight loss increased as the diol ratio of the gels increased. There were two main decomposition steps, one commencing at ~ 250 °C, the other at ~ 475 °C; the final weight loss was completed at 550 °C.

Prefiring the coated substrates for 1 min on a hot-plate set at 350 °C was found to minimize the incidence of macrodefects in the final films. A lower temperature, 300 °C, caused cracks to form, whilst a temperature of 450 °C resulted in many surface holes possibly caused by rapid expulsion of thermolysis products. These results are for coatings deposited at 1500 r.p.m.; higher spin speeds of 3000 and 4000 r.p.m. resulted in less uniform coatings that often exhibited radial striations.

The XRD patterns for films made from stoichiometric starting solutions and then fired for various times at 700 °C are shown in Fig. 3. A crystalline pseudocubic perovskite-type PZT phase (exhibiting preferential (1 1 1) orientation) was dominant in films fired at 700 °C for 5 min, but a pyrochlore phase at 29.5° 2θ was also evident, Fig. 3a. A reduced level of the pyrochlore phase was present in films fired for 15 min, Fig. 3b, with only the perovskite-type phase being detected in films fired for 30 min, Fig. 3c. These samples had been pre-fired for 1 min at 350 °C; it was noted that the pyrochlore phase was more persistent in films prefired for 15 or 30 min and then fired at 700 °C for 30 min. The extent of the pyrochlore phase was also dependent on pre-firing temperature; increasing the hot plate set temperature from 350 °C to 450 °C led to an increased incidence of pyrochlore phase. The diol ratio in the starting sols also affected phase development; decreasing the ratio from 5 to 3 increased the firing times required to produce pyrochlore-free films. It was found that for a diol ratio of 3 the films had to be fired for longer than 30 min at 700 °C to avoid the pyrochlore phase, as opposed to 15–30 min for films made from sols containing a diol ratio of 5.

Expect where stated otherwise, the results reported in the proceedings text are for films prepared using a diol ratio of 5, spun at 1500 r.p.m., prefired for 1 min at a set temperature of 350 °C and fired at 700 °C for 15 min.

A comparison of the XRD patterns of the films prepared from stoichiometric ("0% excess lead") sols

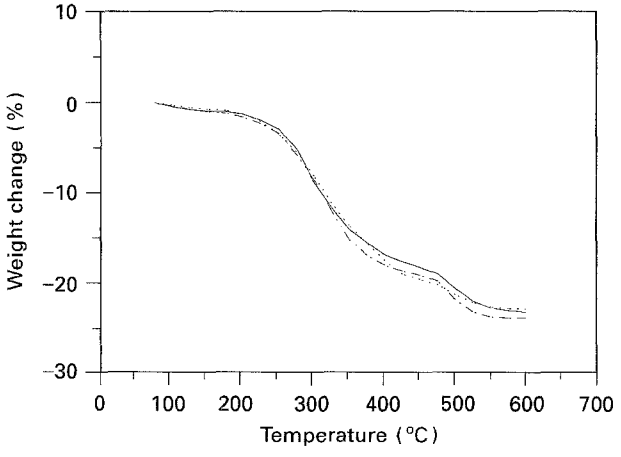

Figure 2 TGA curves of dried gels prepared from sols with different diol ratios: (— · —) 5, (—) 4, (- - -) 3.

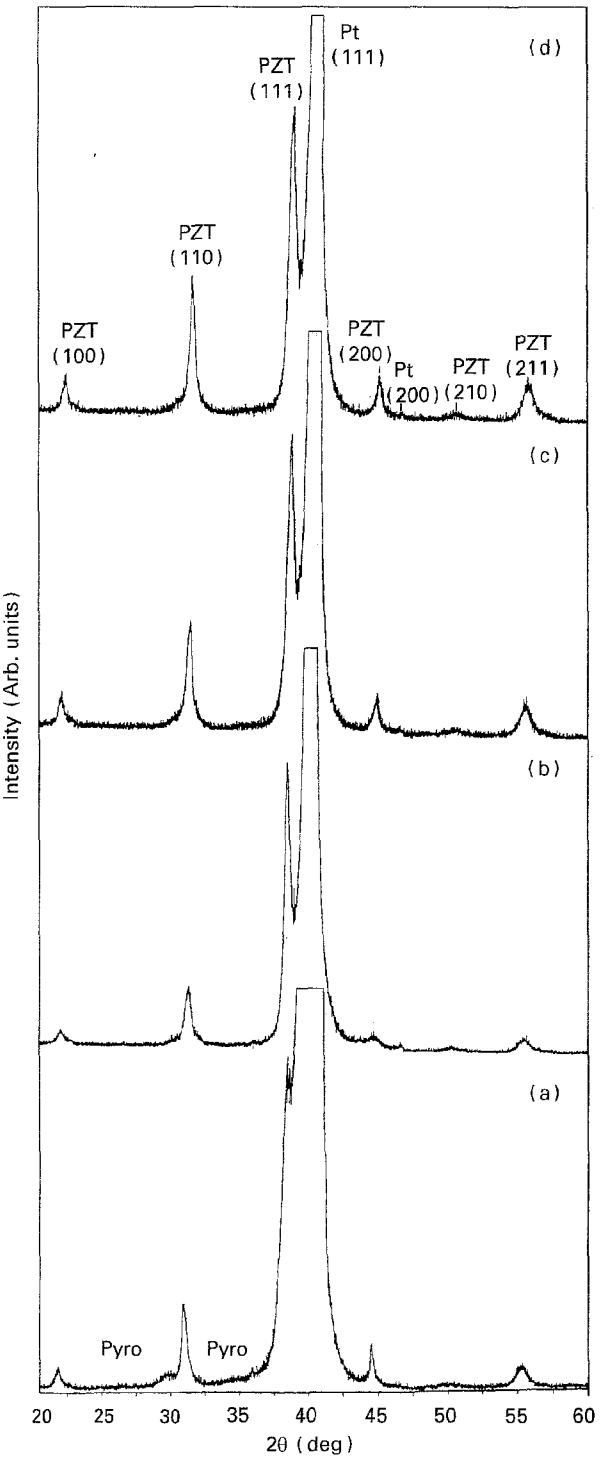

Figure 3 XRD patterns of 0.5 μm PZT stoichiometric films fired at 700 °C for (a) 5 min, (b) 15 min, (c) 30 min, and (d) 1 h.

and those containing 10% and 20% excess lead, all fired for 15 min at 700 °C, are shown in Fig. 4. By using starting sols containing 10 or 20 mol % excess lead acetate it was possible to form single-phase films with no detectable pyrochlore phase, in fact even shorter firing times, e.g. 5 min at 700 °C, were sufficient to form single-phase PZT.

Preferred orientation effects were apparent in all films. The intensity ratio, $\alpha_{1\,1\,1}$, defined as $I_{1\,1\,1}/I_{1\,1\,0} + I_{1\,1\,1}$, decreased from 0.82 for films made from stoichiometric starting sols to 0.53 for sols containing 20 mol % excess $Pb(CH_3COO)_2$, Table I. However, this latter value still indicates a significant degree of (1 1 1) orientation, because for an equivalent powder pattern obtained by calcining bulk gels of the same PZT composition, $\alpha_{1\,1\,1} = 0.15$.

There was also a decrease in XRD peak width for the excess lead samples. This is expressed in relation to the 1 1 0 peak because the 1 1 1 PZT peak partially overlaps with the 1 1 1 peak of the platinum bottom electrode. Values of 1 1 0 half-peak width, B, are presented in Table I. The peak width data may imply an increased crystallite size when excess lead was present in the sols; however, residual strain in the films will also contribute to peak broadening effects and here the variation in B values may also to some extent relate to differences in the degree of strain in the films.

The XRD patterns of films made by depositing stoichiometric PZT sols and applying a PbO precursor sol to help compensate for lead loss during firing (at 700 °C for 15 min) are shown in Fig. 5. Three different concentrations of lead sol were employed, namely 0.4 M, 0.8 M and 1.6 M. No pyrochlore phase was detected in any of the PbO-coated films. There

TABLE I The effect of excess $Pb(CH_3COO)_2$ on preferred orientation, α, and half-peak width, B

	Sol composition		
	0%	10%	20%
$\alpha_{1\,1\,1}$	0.82	0.70	0.53
$B_{1\,1\,0}$ (deg)	0.53	0.39	0.32

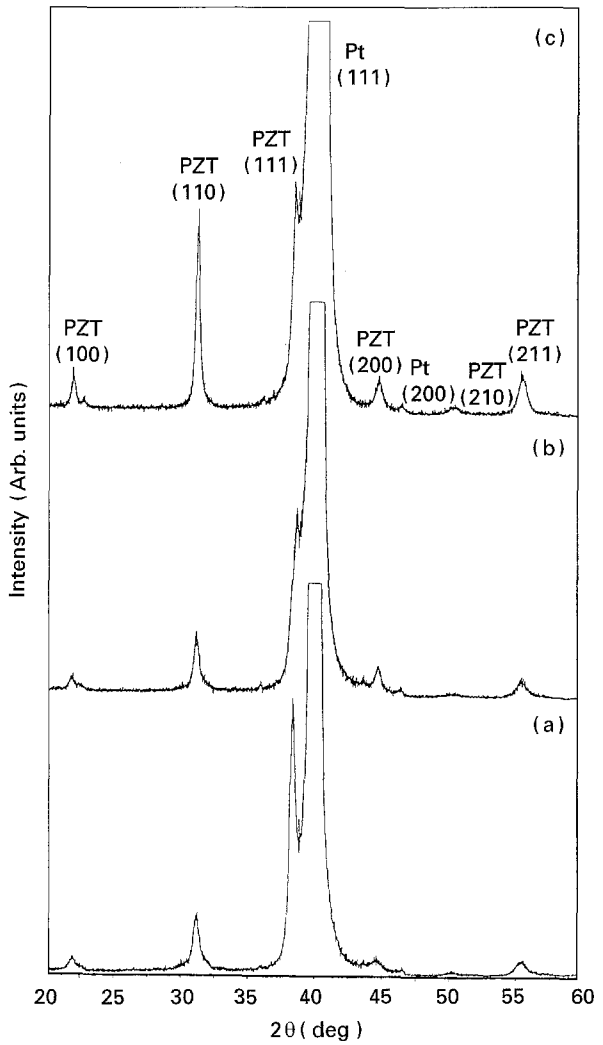

Figure 4 XRD patterns of 0.5 μm PZT films prepared from sols with (a) 0%, (b) 10% and (c) 20% excess lead and fired at 700 °C for 15 min.

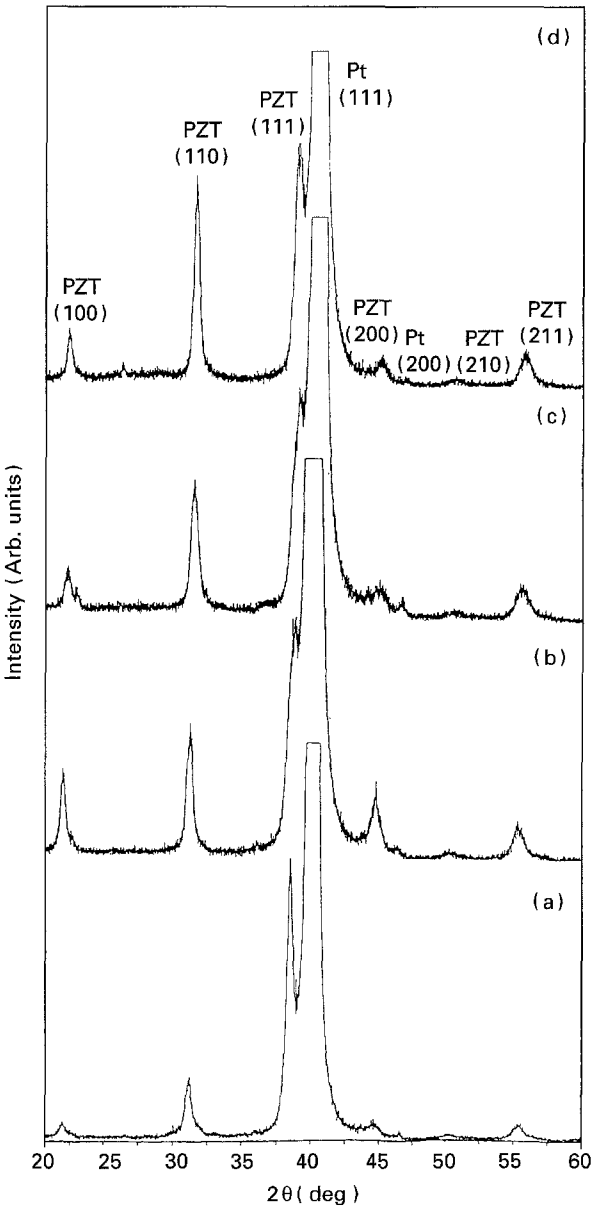

Figure 5 XRD patterns showing the effect of applying a PbO precursor coating to the prefired PZT film. (a) Uncoated, (b)–(d) coated with 0.4 M, 0.8 M and 0.1 M PbO sols, respectively. Films were 0.5 μm thick after firing at 700 °C for 15 min.

was a reduction in the relative intensity of the 1 1 1 peak of the coated samples compared with that of the uncoated film, with α_{111} decreasing to 0.55 when a 1.6 M lead precursor coating was used. This is a similar value to that found above for films made using 20% excess lead sols (Table I). After firing at 700 °C, there was no XRD evidence of residual PbO in any of the films made using the PbO-coating technique, nor in films made using lead excess sols. However, it was present in PbO-coated films fired at lower temperature, e.g. 550 °C. Clearly the vapour pressure of lead oxide at 700 °C was sufficiently high to reduce the excess lead concentration at the surface to below the XRD detection limit.

The 1 0 0 peak of most films fired at 700 °C had a shoulder at ~ 22.7 °2θ which became more pronounced in the 20% excess lead samples and in the PbO-coated films prepared from 0.4 M and 0.8 M precursor sols. An extra peak was also present at 46.3 °2θ; however, this peak also occurs after firing the uncoated substrates and corresponds to the 2 0 0 peak of the underlying platinum electrode, indicating a change in the crystalline state of the platinum electrode during firing.

3.2. Microstructural analysis

The thickness of films prepared by a single deposition of PZT sol, using different sol concentrations, is presented in Fig. 6. A linear relationship between film thickness and molar concentration was observed; selected SEM cross-sections are shown in Fig. 7. Films prepared by concentrating the stock solution to 1.6 M were ~ 1 μm thick, but these concentrated sols occasionally precipitated after standing for > 4 h. Films prepared from 1 M sols were ~ 0.5 μm thick. Interestingly, similar film thickness were obtained when 1 M sols were prepared using a diol ratio of 3 instead of 5 despite the lower measured viscosity of the former. All the films were crack-free, and high-quality surface finishes were observed using optical microscopy.

The microstructures of the surfaces of 0.5 μm PZT films made from 0% and 20% excess lead sols are shown in Fig. 8. For the 0% samples, individual grains < 0.1 μm in size could only be discerned in very localized areas, Fig. 8a; the remainder appeared as microregions (⩽ 0.5 μm in size) of dark and light contrast in which no grains could be resolved using the Hitachi S700. The 10% excess lead microstructure was similar to that of the 0% sample. The 20% excess lead sol yielded a very different microstructure composed entirely of interlocking individual grains up to ~ 0.25 μm in size, Fig. 8b.

The microstructure of a PZT film made using the PbO-coating method is shown in Fig. 9. All three PbO sol concentrations used, 0.4 M, 0.8 M and 1.6 M, exhibited this type of structure composed entirely of ~ 0.1 μm discrete grains.

An examination of the microstructures of films of different thickness, made from 10% excess lead sols of differing concentration, indicated some subtle differences. A 0.25 μm thick PZT film exhibited a more obvious grain structure, Fig. 10a, than did the corresponding 0.5 μm film already described. In the former, ~ 0.1 μm grains were visible over approximately 50% of the surface. Increasing the thickness to 1 μm, Fig. 10b, produced microstructures similar to those of the 0.5 μm films.

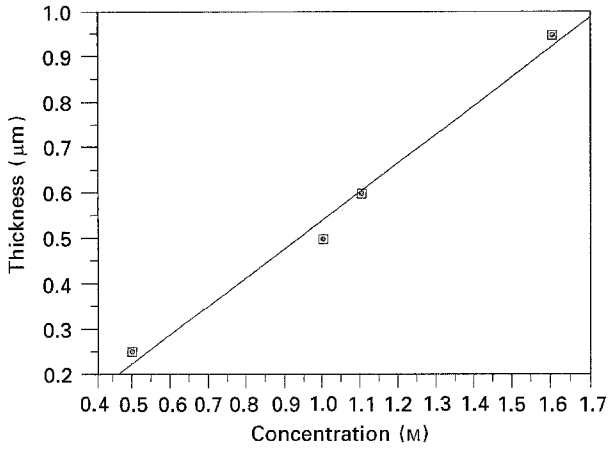

Figure 6 Variation of film thickness with molar concentration of sols.

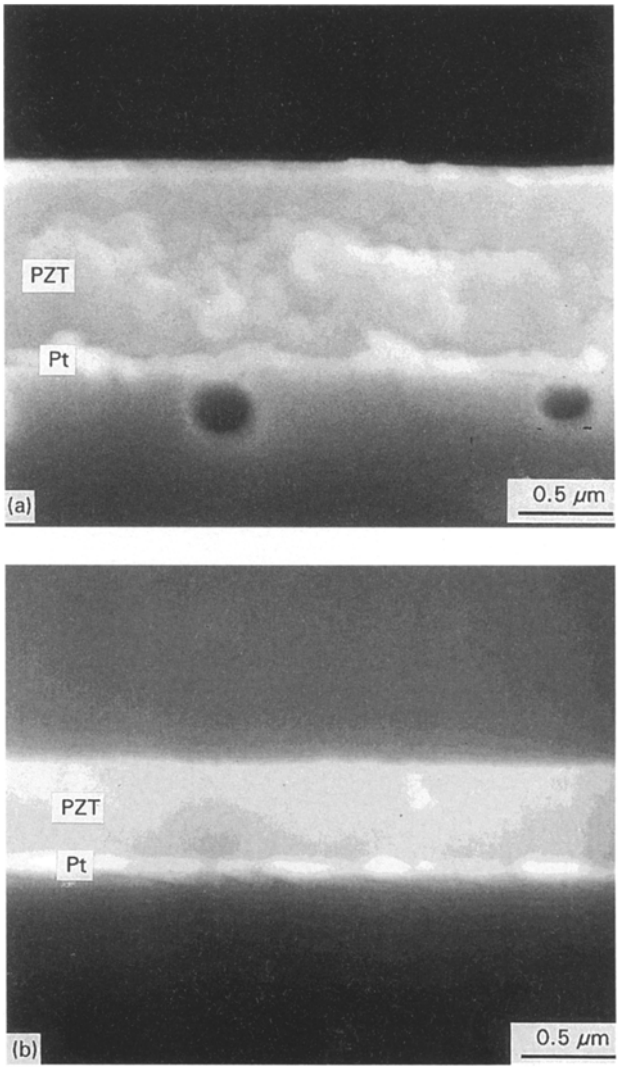

Figure 7 SEM cross-sections of (a) 1 μm and (b) 0.5 μm PZT films.

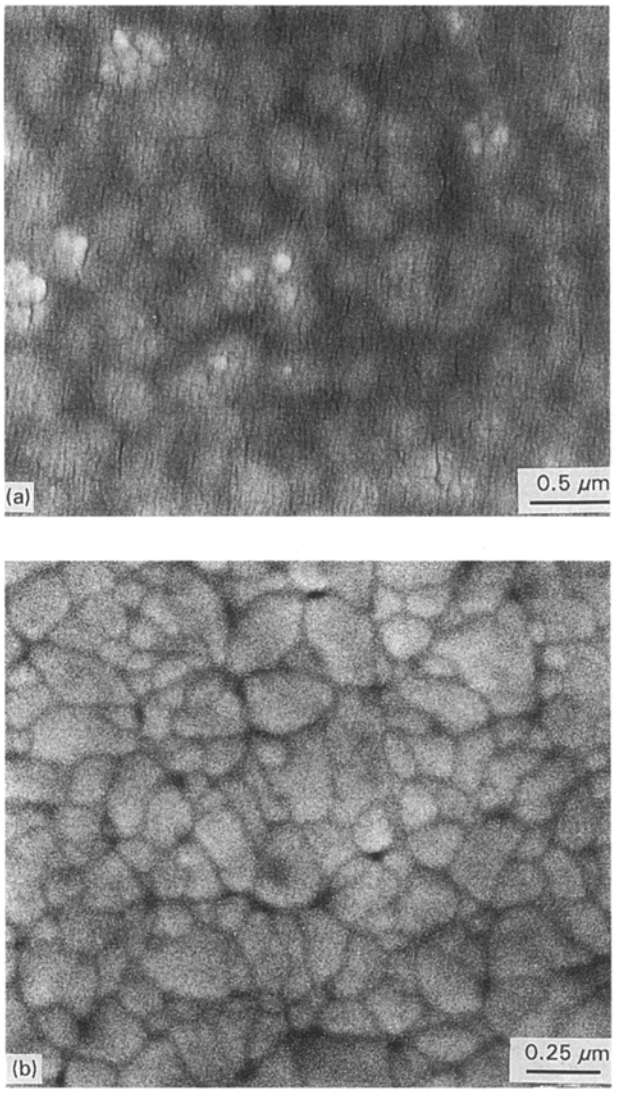

Figure 8 Surface microstructure of 0.5 μm films prepared from sols with (a) 0% and (b) 20% excess lead and fired at 700 °C.

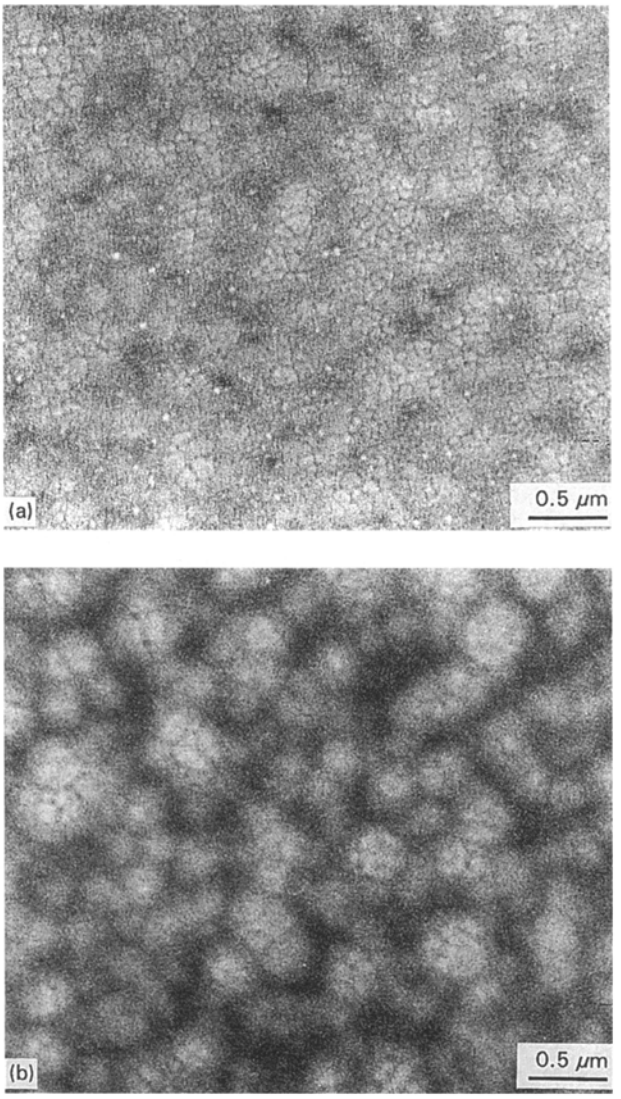

Figure 10 Scanning electron micrographs of top surfaces for (a) 0.25 μm and (b) 1 μm films prepared from sols with 10% excess lead and fired at 700 °C for 15 min.

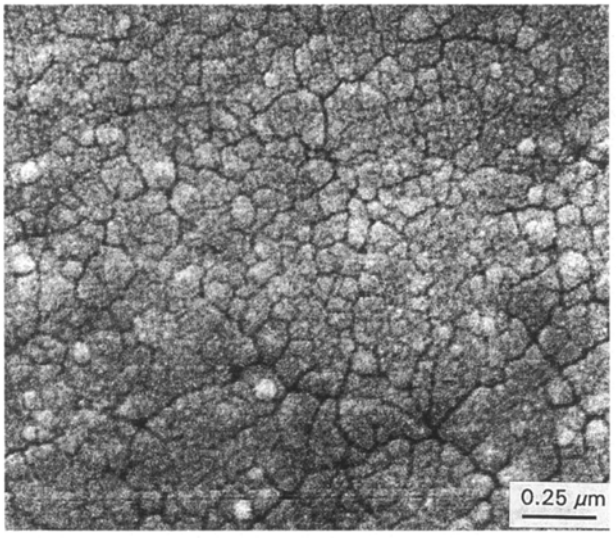

Figure 9 Scanning electron micrographs of a PZT film coated with a PbO precursor sol. The film was fired at 700 °C for 15 min.

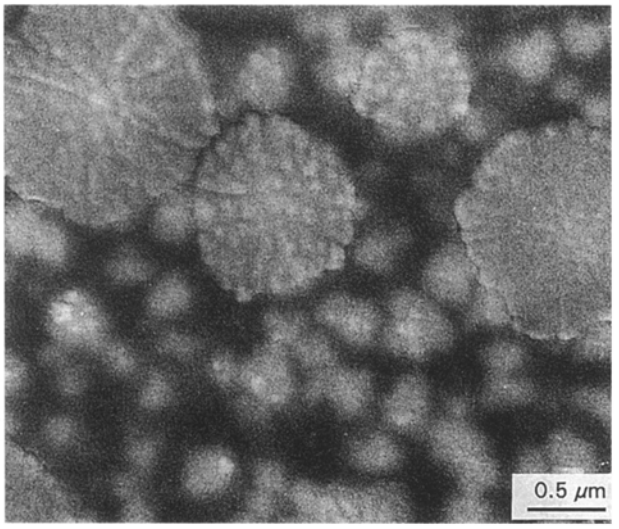

Figure 11 Microstructure of PZT film prepared from stoichiotric sol with a diol ratio 3 and fired at 700 °C for 30 min.

The final microstructure presented is for a 0.5 μm PZT film prepared from a stoichiometric sol synthesized using a diol ratio of 3, instead of 5. This microstructure, Fig. 11, offers a direct comparison to be made with the microstructure shown in Fig. 8a which was for a film fabricated under comparable conditions, but using a diol ratio of 5. The lower diol ratio yielded a classic "rosette" type structure similar

to that reported extensively in the literature for PZT films made by other sol–gel methods [13]. The "rosette" or spherulitic grains were up to 1 μm diameter, and in some there was a clear radial pattern formed by smaller 0.1 μm grains. The remaining microstructure was composed of regions of two distinct contrasts in the SEM, similar in appearance to the microstructure shown in Fig. 8a.

3.3. Electrical properties

The dependence of electrical properties on drying times at 350 °C for the standard 0.5 μm thick films for 30 min at 700 °C is illustrated in Table II. Remanent polarization, P_r, decreased from 13 $\mu C\,cm^{-2}$ to 10 $\mu C\,cm^{-2}$ and relative permittivity, ε_r fell from 400 to 240 when the drying time was increased from 1 min to 1 h. There was a corresponding increase in the coercive field, E_c, from 65 $kV\,cm^{-1}$ at 1 min, to 80 $kV\,cm^{-1}$ after drying for 1 h. Because the aim is eventually to produce films suited to electronic device applications in which high polarization and low coercive fields are generally desirable, a 1 min drying was selected as the standard method.

The electrical properties of the films prepared from solutions containing 0%, 10% and 20% excess lead are compared in Table III. The films were 0.5 μm thick and were fired at 700 °C for 15 min. The value of P_r increased from 14 $\mu C\,cm^{-2}$ to 22 $\mu C\,cm^{-2}$ and E_c decreased from 65 $kV\,cm^{-1}$ to 40 $kV\,cm^{-1}$ with increasing amounts of excess lead, whilst relative permittivity rose from 450 in the 0% sample to 800 in the 20% excess lead sample.

Results for 0.5 μm thick films made from stoichiometric sols using the PbO-coating method are shown in Fig. 12a and b. In general, the coercive field for these samples, 45 $kV\,cm^{-1}$, was intermediate between the 10% and 20% excess lead samples shown in Table III. The measured values of P_r and ε_r were increased by increasing the concentration of the sols used to apply the PbO surface layer. As the concentration increased to 1.6 M, P_r and ε_r reached a value of 27 $\mu C\,cm^{-2}$ and 970, respectively. This compares to measured values of $P_r = 22\ \mu C\,cm^{-2}$ and $\varepsilon_r = 800$ obtained for films made from sols containing 20 mol % excess $Pb(CH_3COO)_2$.

The thickness dependence of the electrical properties of films made from sols of different concentrations, all containing 10% excess $Pb(CH_3COO)_2$, is shown in Fig. 13a and b. Values of E_c were highest for the thinnest 0.25 μm films, decreasing approximately linearly to ~ 40 $kV\,cm^{-1}$ for the ~ 1 μm film. However, there was little variation in P_r with film thickness, Fig. 13a. The ε_r values of the 0.5, 0.6 and 1 μm films showed a rising trend although the ε_r value of the 0.25 μm film was slightly higher than for the 0.5 μm film, Fig.13b.

Examples of the P–E hysteresis loops from which P_r and E_c values were determined are shown in Fig. 14; well-saturated hysteresis loops were obtained for all film thicknesses in the range studied, 0.25–1 μm.

Finally, the electrical properties of 0.5 μm films prepared from stoichiometric 1 M sols with different diol ratios, namely 3 and 5, are compared in Table IV. It can be seen that the films prepared from sols with a diol ratio of 3 further diluted with *n*-propanol had inferior dielectric and ferroelectric properties to films prepared from comparable sols with a diol ratio of 5.

TABLE II Effect of drying times at 350 °C on electrical properties. The 0.5 μm thick films were prepared from stoichiometric solutions and fired at 700 °C for 30 min

Drying time (min)	P_r ($\mu C\,cm^{-2}$)	E_c ($kV\,cm^{-1}$)	ε_r	D
1	13 ± 0.35	65 ± 0.8	400	0.02
30	11 ± 0.18	75 ± 0	300	0.04
60	10 ± 1	80 ± 0.8	240	0.03

TABLE III The effect of using sols with excess $Pb(CH_3COO_2)_2$ on the electrical properties of 0.5 μm films fired at 700 °C for 15 min

PZT sol composition	P_r ($\mu C\,cm^{-2}$)	E_c ($kV\,cm^{-1}$)	ε_r	D
0% excess Pb	14 ± 0.4	65 ± 0.8	450	0.02
10% excess Pb	16 ± 0.7	50 ± 0.8	630	0.02
20% excess Pb	22 ± 0.6	40 ± 0.8	800	0.03

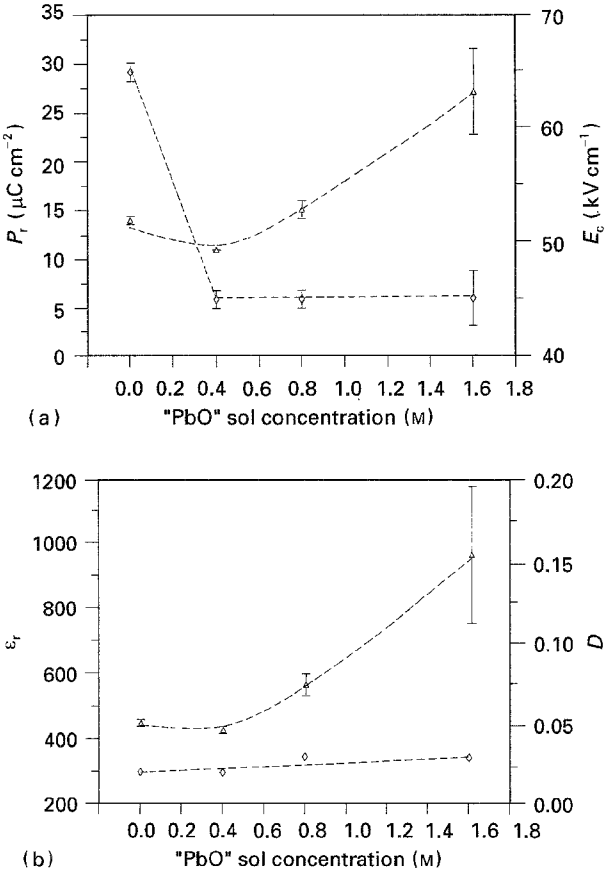

Figure 12 Comparison of (a) (△) P_r and (◇) E_c, (b) (△) ε_r and (◇) D of PZT films coated with a lead oxide surface layer deposited using different concentrations of the coating solution. Films were fired at 700 °C for 15 min.

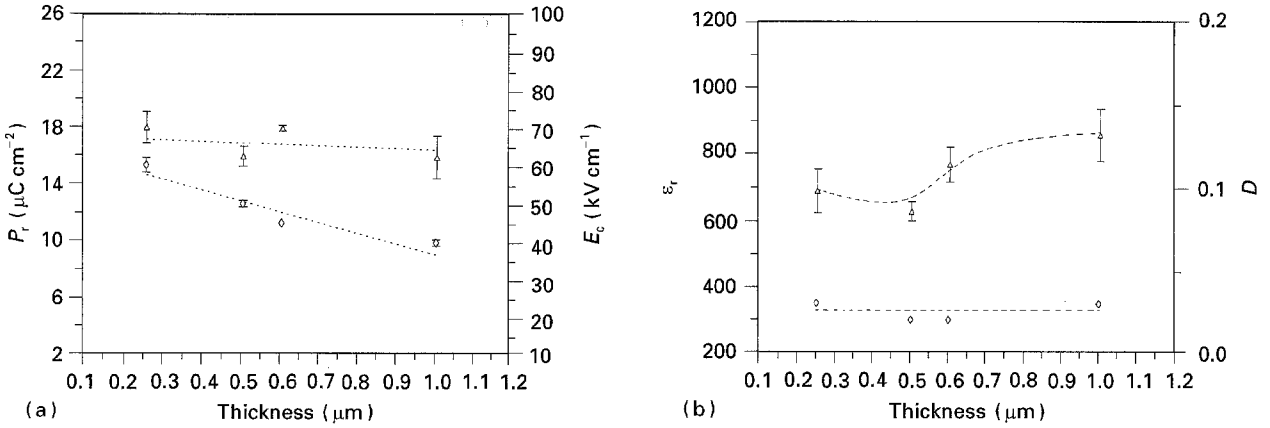

Figure 13 Thickness dependence of (a) (△) P_r and (◇) E_c, (b) (△) ε_r and (◇) D for the films prepared from sols with 10% excess lead and fired at 700 °C for 15 min.

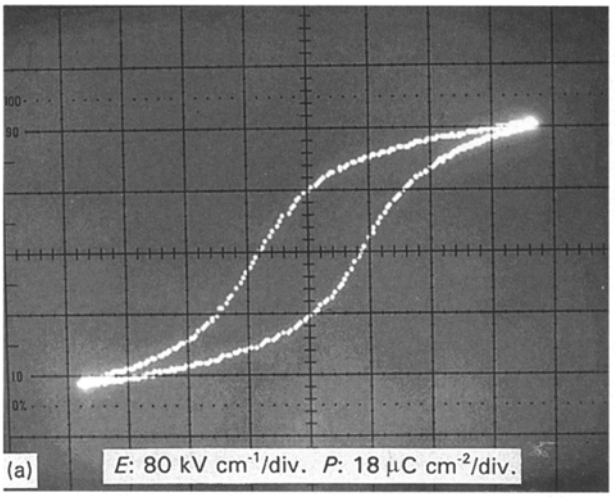

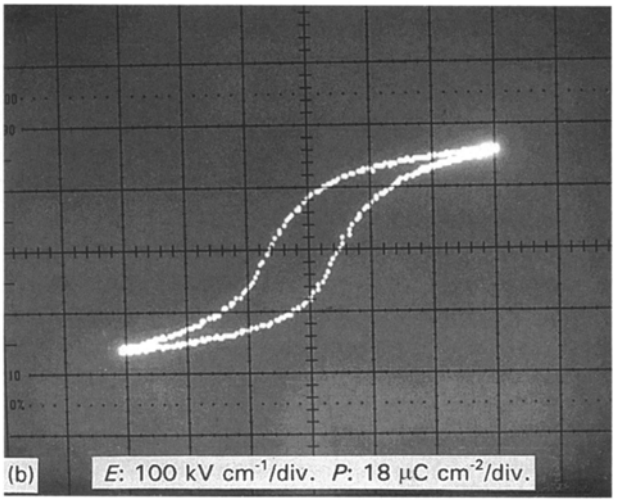

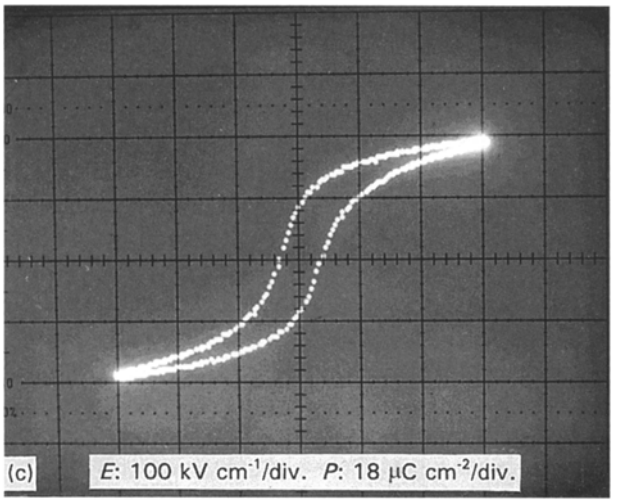

Figure 14 P–E hysteresis loops for (a) 0.25 μm, (b) 0.5 μm and (c) 1 μm films prepared from sols containing 10% excess lead and fired at 700 °C for 15 min.

TABLE IV Effect of diol ratio on electrical properties of the films prepared from stoichiometric starting sols. Films were fired at 700 °C for 30 min

Diol ratio	P_r (μC cm^{-2})	E_c (kV cm^{-1})	ε_r	D
3	7 ± 1.4	60 ± 3.0	250	0.05
5	13 ± 0.35	65 ± 0.8	400	0.02

4. Discussion

It is apparent that a single-layer PZT film up to 1 μm thick can be obtained using our diol-based route. This corresponds to an approximately ten-fold increase in single layer thickness compared to the popular methoxyethanol sol–gel process [4]. As stated in Section 1, another route based on acetic acid would seem to offer a similar single-layer thickness to the diol route [5]; however, other workers have suggested that the practical limiting single-layer thickness of PZT deposited from acetic acid solutions on platinized silicon is actually ~ 0.2 μm [6]. However, for both methoxyethanol and acetic acid systems, thicker films can be built up using multiple deposition techniques. For methoxyethanol systems we have found that the maximum thickness that can be built up using hot-plate intermediate heat treatments between coatings is 1 μm, requiring up to ten repeated coatings.

The nominal film composition studied here, $PbZr_{0.53}Ti_{0.47}O_3$, is close to the morphotropic phase boundary separating tetragonal from rhombohedral PZT solid solutions. The product phase identified on our XRD pattern is thus best described as pseudocubic although it is often loosely referred to as perovskite. Unfortunately, the characteristically broad XRD peaks of the films prevented further analysis as to their rhombohedral/tetrahedral phase content(s).

The additional pyrochlore phase present in a number of our films, especially those prepared using high hot-plate temperatures, low firing temperatures and/or short firing times, is a common intermediate in sol–gel derived PZT. It has been suggested that the existence of this pyrochlore phase is promoted by lead deficiency. Thus, pyrochlore may be expected to occur predominantly at the surface of the films [14] because some PbO loss by volatilization is inevitable at the firing temperature used, 700 °C, especially given the high surface area/volume ratio of thin films. Hence films made from stoichiometric starting sols will probably be lead-deficient to some degree. Our experimental data illustrate the close relationship between assumed lead stoichiometry and pyrochlore formation. We have confirmed that the tendency for pyrochlore formation in the fired films is reduced significantly by incorporating sufficient excess lead into the starting sols or by coating the pre-fired films with a PbO precusor sol [15].

Excess lead also led to sharper XRD peaks, possibly indicating an increased crystallite size or reduced strain in the films. Other workers suggest that excess lead promotes grain growth in PZT thin films made by other sol–gel routes [16]. Our microstructures for 20 mol % excess lead sols and PbO-coated films also show an increased grain size.

Different processing conditions brought about interesting trends in preferred orientation. All films exhibited a preferential alignment of the (1 1 1) planes parallel to the film surface, although the relative 1 1 1 peak intensity was closely dependent on processing conditions. The orientation effect is consistent with the (1 1 1) orientation of the underlying platinum layer. The change in orientation brought about by the presence of excess lead either in the starting sol or applied using a surface lead coating implies different crystallization mechanisms compared to the case of uncompensated films. TEM investigations by Tuttle *et al.* [14] indicated two forms of PZT crystallites in films made by another sol–gel route and fired at > 650 °C. One type had a rosette morphology which was proposed to originate from heterogeneous nucleation at the platinum interface. The other was composed of dense grains smaller than 0.5 μm which they suggested to be due to homogeneous nucleation, presumably within the bulk of the film. It may be that the latter type of grains are present in our PZT films in which lead loss has been compensated for; these films exhibit less (1 1 1) preferred orientation than do other non-compensated samples which is consistent with the (1 1 1) platinum interface having less bearing on crystallite nucleation and growth. Crystallization to perovskite PZT in lead-deficient or stoichiometric samples may be more difficult; heterogeneous nucleation at the platinum interface would thus play a more dominant role in the overall crystallization process and lead to more orientation, as found experimentally. However, more detailed studies of microstructures and orientation effects are required before a detailed explanation of the present experimental results can be presented.

The unidentified shoulder or peak at 22.7° 2θ was found for most films fired at 700 °C. Interestingly all films which showed this extra peak also exhibited a Pt(2 0 0) peak. Others have found the same extra 1 0 0 peak shoulder [17] and attributed it to the inter-rosette phase (see Fig. 8a). The development of a Pt(2 0 0) peak in heat-treated films has also been reported in the literature [18].

Film microstructures were closely dependent on lead composition. For samples prepared from stoichiometric starting sols or sols containing 10 mol % excess lead it was generally difficult to resolve any grain structure in most areas of the film using SEM. The scanning electron micrographs of the films showed regions of dark and light contrast which may signify local variations in lead content. In some cases, e.g. the 0.25 μm film, ~ 0.1 μm grains could be distinguished in regions of light contrast. Many papers on PZT (53/47) films prepared from sol–gel routes report a rosette-type structure in which rosette-like or spherulitic grains co-exist with a very fine-grained matrix [13, 14, 19]. The former are often interpreted to be a perovskite phase and the fine-grained fraction a pyrochlore phase. Workers using TEM–EDX techniques have demonstrated the fine-grained phase to be lead-deficient and they assigned it to be a pyrochlore phase [20].

Assuming this to be the case, the preponderance of a fine-grained structure in our 0% and 10% excess lead films would imply considerable lead-deficiency, but this may be limited to a thin surface layer because often the films did not exhibit any detectable pyrochlore phase in XRD traces. The larger grain size of 20 mol % excess lead and PbO-coated samples implies no surface pyrochlore phase and is probably an indirect consequence of differences in crystallization processes brought about by changes in lead stoichiometry.

The microstructural differences arising from different diol ratios may be indicative of different gel structures and solvent loadings, giving rise to different crystallization mechanisms. In previous studies we have found that heating rates are much more important than firing times or dwell temperatures (in the range 550–700 °C) in determining PZT film microstructures. Film microstructures we believe are essentially a crystallization product and not strongly influenced by normal sintering mechanisms. It is thus reasonable to expect that gels made with different proportions of diol and propanol crystallize in slightly different ways and hence show different microstructures. Slight changes to solution processing conditions for other sol–gel routes have also been reported to affect the microstructure of PZT films [21, 22].

Dielectric and ferroelectric properties showed a strong correlation with lead compensation, the presence of pyrochlore phase and film microstructures. For example, the electrical properties of films with different lead starting stoichiometries indicated that P_r and ε_r were both highest and E_c lowest for films made from sols with 20 mol % excess lead, and in films treated with a PbO surface layer. The manner in which lead loss was compensated for seemed to have little influence on electrical properties; adding 20 mol% excess $Pb(CH_3COO)_2$ to the starting sols or

applying a PbO coating using 1.6 M precursor sols both enhanced ferroelectric and dielectric properties to a similar degree. The superior P_r and ε_r properties of these films may be due to the absence of a lead depletion surface layer and to an absence of residual pyrochlore phase compared to other films. The nature of the crystallite preferred orientation, or texture, also influenced electrical properties; properties generally improved with decreasing (1 1 1) orientation.

An absence or reduction in non-ferroelectric pyrochlore crystallites in excess lead systems may in part lower E_c values, because any pyrochlore phase would reduce the local effective applied field on the major ferroelectric component leading to higher switching voltages. However, microstructural evidence suggests that the increased grain size in excess lead systems may also account for their lower E_c values. The larger variation in electrical parameters for the films carrying a surface coating prepared from the most concentrated 1.6 M precursor sol, Fig. 12, could indicate incomplete volatilization of the surface PbO coating in regions of the film.

The changes in electrical properties with increasing film thickness probably arise due to several factors. For example, a reduced level of strain in thicker films [6] and a reduced proportion of any surface pyrochlore phase [23] would both be expected to lead to lower coercive fields, as measured experimentally. Similar arguments could be applied to relative permittivity values in the range 0.5–1 μm, although the reduction in permittivity from 0.25 μm to 0.5 μm is rather surprising. Possibly the slightly different microstructures of the latter two samples may be significant in this respect. Our trends in E_c and ε_r values are generally similar to results reported for multiple-coated films made from methoxyethanol [23] and acetic acid routes [24]. However, other workers have found, in contrast to our results, that P_r increases with increasing film thickness [23, 24].

5. Conclusions

The diol sol–gel method enables PZT films up to 1 μm thick to be prepared from a single coating on platinized silicon substrates. Although there are a number of process variables to be controlled in order to produce good-quality coatings, our experimental results imply that control of the lead content is imperative in order to produce films exhibiting favourable dielectric and ferroelectric properties. This can be achieved by either incorporating excess lead acetate into the starting sol, or by applying a lead oxide precursor sol to the pre-fired film. Using the latter technique, PZT (53/47) films having a P_r of $\sim 27\ \mu C\,cm^{-2}$, E_c value of $\sim 45\ kV\,cm^{-1}$ and ε_r of ~ 1000, can be produced.

Acknowledgements

We thank R. W. Holt for helpful discussions. Y. L. Tu thanks the ORS Award Scheme for financial support.

References

1. J. FUKUSHIMA, K. KODAIRA and T. MATSUSHITA, *J. Mater. Sci.* **19** (1984) 595.
2. J. BLUM and S. GURKOVICH, *ibid.* **20** (1985) 4479.
3. K. D. BUDD, S. K. DEY and D. A. PAYNE, *Br. Ceram. Proc.* **36** (1985) 107.
4. S. H. PYKE, PhD thesis, University of Leeds (1990).
5. G. YI, Z. WU and M. SAYER, *J. Appl. Phys.* **64** (1988) 2713.
6. C. K. KWOK, S. B. DESU and D. P. VIJAY, *Ferroelect. Lett.* **16** (1993) 143.
7. N. J. PHILLIPS, M. L. CALZADA and S. J. MILNE, *Br. Pat. Appl.* 9114476.6 (1991).
8. *Idem, J. Non-Cryst. Solids* **147/148** (1992) 285.
9. M. L. CALZADA and S. J. MILNE, *J. Mater. Sci. Lett.* **12** (1993) 1221.
10. S. J. MILNE and S. H. PYKE, *J. Am. Ceram. Soc.* **74** (1991) 1407.
11. M. GUGLIELMI and G. CARTURAN, *J. Non-Cryst. Solids* **100** (1988) 16.
12. D. C. BRADLEY, R. C. MEHROT and D. P. GAUR, "Metal Alkoxides" (Academic Press, London, 1978).
13. S. A. MYERS and L. N. CHAPIN, *Mater. Res. Soc. Symp. Proc.* **200** (1990) 231.
14. B. A. TUTTLE, T. J. HEADLEY, B. C. BUNKER, R. W. SCHWARTZ, T. J. ZENDER, C. L. HERNANDEZ, D. C. GOODNOW, R. J. TISSOT, J. MICHALE and A. H. CARIM, *J. Mater. Res.* 7 (1992) 1876.
15. T. TANI and D. A. PAYNE, *J. Am. Ceram. Soc.* **77** (1994) 1242.
16. G. TEOWEE, J. M. BOULTON and D. R. UHLMANN, *Mater. Res. Soc. Symp. Proc.* **271** (1992) 345.
17. G. A. C. M. SPIERINGS, M. J. E. ULEANERS, G. L. M. KAMPSCHOER, H. A. M. van HAL and P. K. LARSEN, *J. Appl. Phys.* **70** (1991) 2290.
18. G. A. C. M. SPIERINGS, J. B. A. VAN ZON, P. K. LARSEN and M. KLEE, *Integ. Ferroelect.* **3** (1993) 283.
19. A. H. CARIM, B. A. TUTTLE, D. H. DOUGHTY and S. L. MARTINEZ, *J. Am . Ceram. Soc.* **74** (1991) 1455.
20. I. M. REANEY, K. BROOKS, R. KLISSURSKA, C. PAWLACZYK and N. SETTER, *ibid.* **77** (1994) 1209.
21. C. D. E. LAKEMAN and D. A. PAYNE, *ibid.* **75** (1992) 3091.
22. R. W. SCHWARTZ, B. C. BUNKER, D. B. DIMO, R. A. ASSINK, B. A. TUTTLE, D. R. TALLANT and I. A. WEINSTOCK, in "Proceedings of the 3rd International Symposium on Integrated Ferroelectrics" (1991) pp. 535–46 (C.A. Paz de Araajo, Colorado Spring, Colorado, USA).
23. K.AMANUMA, T. MORI, T. HASE, T. SAKUMA, A. OCUI and Y. MIYASAKA, *Jpn J. Appl. Phys.* **32** (1993) 1150.
24. G. YI, Z. WU and M. SAYER, *Ceram. Trans.* **11** (1990) 363.

Received 16 August
and accepted 10 October 1994